Proceedings of the 2018 IEEE International
Conference on Intelligence and Safety for Robotics
Shenyang, China, August 24-27, 2018

Robust and Safe Control of a Knee Joint Orthosis

Guangzheng Ding, Weiguang Huo, Jian Huang, Yacine Amirat and Samer Mohammed

Abstract— **This paper concerns the control of a knee joint orthosis for rehabilitation and assistive purpose. The dynamics of shank-orthosis system can be represented as a second order nonlinear model which takes viscous, inertial and gravitational properties into consideration and the human effort is considered as an external torque. In this paper, an adaptive proxy-based sliding mode control (APSMC) is proposed to guarantee an accurate and robust tracking performance of shank-orthosis system. The main advantages of this control law are 1) on-line parameters regulation which ensures a better tracking performance and robustness with respect to parameter uncertainties and external disturbance. 2) the safety of the robot is guaranteed in the presence of a large tracking error which results from the abnormal operation. The effectiveness of the APSMC is verified by comparison with three control methods, PID control, adaptive PID control and traditional proxy-based sliding mode control, in the real-time experiments using knee orthosis with two healthy subjects. The experiment results show that APSMC improves tracking accuracy and robustness. Last but not least, the intrinsic safety is guaranteed by APSMC.**

I. INTRODUCTION

The wearable rehabilitation robot has drawn a great deal of interest related to the increase of the disabled and elderly. Wearable robots are devices equipped with sensors gathering information about the limbs posture, muscles' activity, etc. The information is used in the controller to produce control signal for driving the actuators that accomplish a desired trajectory which can be a pre-defined one for clinic requirement or computed instantaneously with respect to the wearer intention.

Knee orthoses are used to help patients who suffer damaged limb functions at knee joint level due to a stroke, spinal cord or traumatic injuries to regain the ability to control their limbs. Compared to traditional non-robotic physical therapies, knee joint orthosis has the advantage of smooth, continuous and repeatable movement of the knee joint in clinical environment. Some designs of knee joint orthoses have been presented in the following. In [1], the orthosis RoboKnee is used to assist the thigh muscles during movements. The users intention is dependent on the measurement of the vertical ground reaction force. The controller is considered as an amplifier as the actuator torque is proportional to the desired one. In [2], an orthosis is designed to reduce the joint stiffness and increase the flexion/extension range of motion. The cyberthosis [3][4] is used to train the muscles and knee joint for flexion/extension movements by a PID controller.

The dynamics of the shank-orthosis system can be represented as a nonlinear second order model. Many control strategies of knee joint orthoses have been proposed. In [5], a terminal sliding mode controller with the nonlinear observer is designed to improve the tracking performance and robustness of the shank-orthosis system. In [6], an observer-based active impedance control is developed to decrease the impedance of the shank-orthosis system to a desired level. In [7], a model reference adaptive control law allows on-line parameter regulation to ensure the best tracking performance. One should emphasize that none of the aforementioned control methods concerned the safety issue. Intrinsic safety is crucial for any rehabilitation robots which interact with humans directly [8]. A violent and unsafe response of the human-robot system may be produced following a large position error and may cause physical damages to the wearer.

This is different in the case of proxy-based sliding mode control (PSMC), which is proposed by Kikuuwe and Fujimoto [9]. The principle of PSMC is the introduction of a virtual object, called proxy, which is controlled by a conventional sliding mode controller (SMC). And the proxy is connected with the end effector by a PID type virtual coupling. In this way, the discontinuous signum function in SMC is replaced by a saturation function, which is able to avoid the chattering problem in SMC. Thus, PSMC can be viewed as a combination of traditional SMC and PID control . It inherits the intrinsic safety of SMC but without the disadvantage of chattering [10]. However, the best tracking performance the PSMC can achieve is like PID control [11], which is not satisfactory for knee orthosis control.

Since the shank-orthosis system parameters vary from subject to other and human effort (external disturbance) is difficult to measure [12], the PSMC is not robust enough to maintain its tracking performance. This paper proposes a new adaptive proxy based sliding mode control (APSMC) applied to the knee orthosis by introducing an adaptation interaction method [13], which allows online tuning of the PID gains in the PSMC scheme. Therefore, the proposed APSMC is more adaptive to the changes in the system's dynamics and external disturbances, while providing a better tracking performance with respect to the standard PSMC. At mean time, the benefit of safety is preserved in APSMC.

*This work was supported by the National Natural Science Foundation of China under Grant 61473130, and the Beijing Advanced Innovation Center of Intelligent Robots and Systems under Grant 2016IRS10.

Weiguang Huo, Yacine Amirat, Samer Mohammed are with Laboratoire Images, Signaux et Systèmes Intelligents (LISSI), Université Paris-Est Créteil (UPEC), 94400 Vitry-sur-Seine, France. e-mail weiguang.huo@u-pec.fr

Guangzheng Ding, Jian Huang are with Key Laboratory of Ministry of Education for Image Processing and Intelligent Control, School of Automation, Huazhong University of Science and Technology, Wuhan, Hubei, 430074 P.R. China.

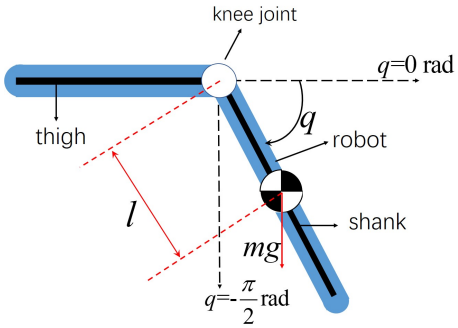

Fig. 1. Representation of the equivalent system.

II. SYSTEM MODELING

The system model composed of the human shank and the embodied knee joint orthosis is shown in Fig. 1. In the following, the subscripts s and o represent the shank and orthosis, respectively. According to the Lagrange formulation, the system's dynamics can be described as follows:

$$J\ddot{q} = -\tau_g \cos q - A\text{sgn}\dot{q} - B\dot{q} - K(q - q_r) + \tau + \tau_h, \quad (1)$$

where q denotes the knee joint angle between shank and thigh direction. $J = J_s + J_o$ denotes the sum of inertia of shank and orthosis. $\tau_g = (m_s l_s + m_o l_o)g$ denotes the shank-orthosis system gravity torque. $A = A_o$ and $B = B_s + B_o$ represent the solid and viscous friction parameters of shank-orthosis system, respectively. $K = K_s$ the stiffness coefficient, q_r the rest position of the knee joint, τ_h the skeletal muscular torque actuating the knee joint and τ the input torque generated by actuator. $\text{sgn}()$ is the signum function. The system internal and external torques are considered as disturbances to the system. Therefore, (3) can be rewritten as:

$$J\ddot{q} + B\dot{q} + Kq = f + d, \quad (2)$$

with

$$d = -\tau_g \cos q - A\text{sgn}\dot{q} + Kq_r + \tau_h \quad (3)$$

where $f = \tau$, and d represents all the non-linear parts and external disturbances.

III. CONTROLLER DESIGN

A. PSMC Principle

The basic idea of PSMC is the introduction of an imaginary object, called a proxy, which is connected with the actual controlled object through a PID-type virtual coupling. The proxy is controlled by a sliding mode controller so that the proxy position can track the desired position, while the end effector position can track the proxy position with PID controller. The control signal exerted by the SMC is given by:

$$F_{smc} = F\text{sgn}(s), \quad (4)$$

where

$$s = q_d - p + H(\dot{q}_d - \dot{p}) \quad (5)$$

with q_d, $\dot{q}_d$ the desired position and velocity, respectively; p, $\dot{p}$ the proxy position and velocity, respectively. $F > 0$ and $H > 0$ are the designed parameters. After the proxy reaches the sliding surface, i.e. $s = 0$, the error dynamics is determined by:

$$\dot{e}_p + \frac{1}{H}e_p = 0 \quad (6)$$

where $e_p = q_d - p$. Thus the proxy position exponentially converge to the desired position. The PID virtual coupling is given by:

$$F_{pid} = K_p e_q + K_i \int_0^t e_q d\tau + K_d \dot{e}_q, \quad (7)$$

with

$$e_q = p - q. \quad (8)$$

By defining

$$a = \int_0^t (p - q)d\tau \quad (9)$$

and

$$\sigma = q_d - q + H(\dot{q}_d - \dot{q}), \quad (10)$$

(4) and (7) can be expressed as:

$$F_{smc} = F\text{sgn}(\sigma - \dot{a} - H\ddot{a}) \quad (11)$$

and

$$F_{pid} = K_p\dot{a} + K_i a + K_d\ddot{a}. \quad (12)$$

The dynamics of the proxy is given by:

$$m_p\ddot{p} = F_{smc} - F_{pid}, \quad (13)$$

where m_p is proxy mass. Since m_p can be set to zero, we have $F_{smc} = F_{pid} \equiv f$. Therefore, the PSMC law is given as:

$$f = F\text{sgn}(\sigma - \dot{a} - H\ddot{a}) = K_p\dot{a} + K_i a + K_d\ddot{a}. \quad (14)$$

The following formulation is derived from (14), according to the relationship between signum function and saturation function [11]:

$$\ddot{a} = -\frac{K_p\dot{a} + K_i a}{K_d} + \frac{F}{K_d}\text{sat}\left(\frac{K_d}{F}\left(\frac{\sigma - \dot{a}}{H} + \frac{K_p\dot{a} + K_i a}{K_d}\right)\right). \quad (15)$$

Substitute (15) into (14), the PSMC control law can be expressed as follows:

$$f = F\text{sat}\left(\frac{K_d}{F}\left(\frac{\sigma - \dot{a}}{H} + \frac{K_p\dot{a} + K_i a}{K_d}\right)\right). \quad (16)$$

The equivalent control block is shown in Fig. 2(a).

B. Design of the APSMC

Since the tracking performances of PSMC are largely affected by the parameter uncertainties of the model (1) as well as the external disturbance, the fixed PID control gains is not satisfying for the control of the knee orthosis. The proposed APSMC introduces an adaptive algorithm to the traditional PSMC so that the three PID gains are self-tuning parameters. The diagram of APSMC is shown in Fig. 2(b). By applying the adaptive interaction method [13] to the PID

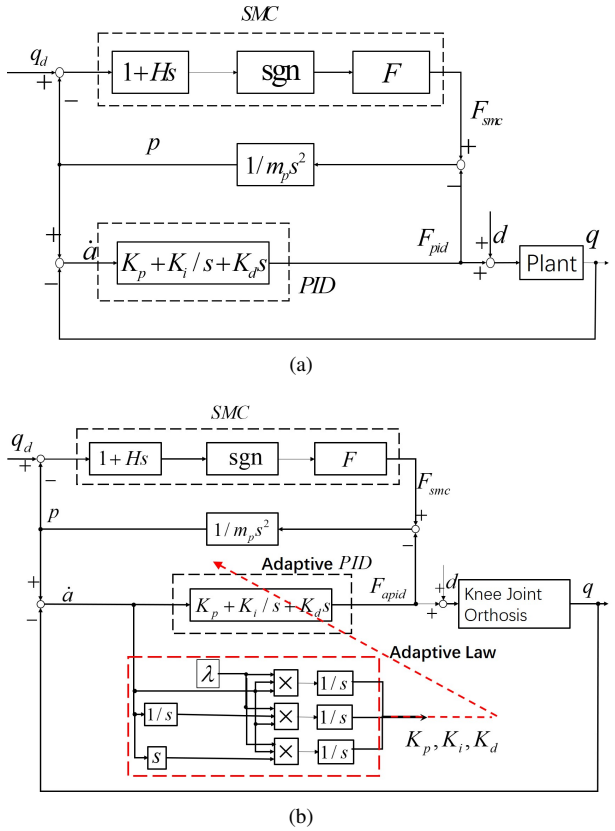

Fig. 2. Control block of two PSMCs. (a)Conventional PSMC control block. (b)APSMC control block.

type virtual coupling, the adaptive law of the PID control gains can be written as:

$$\begin{cases} \dot{K}_p = -\gamma \frac{\partial E}{\partial y} \circ \dot{G}[u] \circ c_1 \\ \dot{K}_i = -\gamma \frac{\partial E}{\partial y} \circ \dot{G}[u] \circ c_2 \\ \dot{K}_d = -\gamma \frac{\partial E}{\partial y} \circ \dot{G}[u] \circ c_3 \end{cases}, \tag{17}$$

where γ denotes the adaptation gain. y denotes the plant's output. c_1, c_2, c_3 represent the output of the proportional, the integral and the derivative subsystems, respectively. G describes the mapping function between the plant's input and output:

$$y(t) = G[u](t) = (G \circ u)(t). \tag{18}$$

$\dot{G}[u]$ represents the Frechet derivative of G, which satisfies:

$$\lim_{\|\Delta\| \to 0} \frac{\left\| G[u+\Delta] - G[u] - \dot{G}[u]\Delta \right\|}{\|\Delta\|} = 0. \tag{19}$$

E denotes the performance index:

$$E = e_a^2 = (y_d - y)^2 \tag{20}$$

with y_d the plant's desired input. For the system (1), the Freche derivative can be approximated by [14]:

$$\dot{G}[u] \circ h \approx \beta h \tag{21}$$

where β is a constant. Therefore, the adaptive algorithm (17) becomes:

$$\begin{cases} \dot{K}_p = \lambda e_a c_1 \\ \dot{K}_i = \lambda e_a c_2 \\ \dot{K}_d = \lambda e_a c_3 \end{cases}. \tag{22}$$

where $\lambda = 2\gamma\beta$.

By applying (22) to proxy-based sliding mode controller, the desired input to adaptive PID controller is $y_d = p$ and output is $c_4 = q$. Considering (9), we have: $e_a = y_d - c4 = p - q = \dot{a}$, $c_1 = e_a = \dot{a}, c_2 = \int e_a d\tau = a, c_3 = \dot{e}_a = \ddot{a}$. Thus, the adaptive law for APSMC is given by:

$$\begin{cases} \dot{K}_p = \lambda \dot{a} a \\ \dot{K}_i = \lambda \dot{a} a \\ \dot{K}_p = \lambda \dot{a} \ddot{a} \end{cases}. \tag{23}$$

C. Stability Analysis

Define the tracking error $e = q_d - q$ and the error vector as:

$$E = [e \quad E_1] \tag{24}$$

where $E_1 = [\dot{e} \ \dot{a} \ a]$. By substituting (24) to (2), the error dynamics equation is obtained:

$$J\ddot{e} + B\dot{e} + Ke = -f + \varphi, \tag{25}$$

with

$$\varphi = J\ddot{q}_d + B\dot{q}_d + Kq_d - d, \tag{26}$$

where $|\varphi| \leq \delta_0$ with $\delta_0 > 0$. To demonstrate the stability of the APSMC for the system (25), the following lemma is introduced.

Lemma 1 ([11]): Considering the closed-loop system composed of system (25) and an adaptive PID controller (12) and (23) that accepts an input $u = \dot{p} - \dot{q}_d$, there exists K_p, K_i, K_d that allow that the function V_p satisfies:

$$V_p(E_1) \geq \delta \|E_1\|^2, \tag{27}$$

and

$$\dot{V}_p(E_1) \leq fu - \rho_E \|E_1\|^2 - \rho_u \|u\|^2, \tag{28}$$

where ρ_E, ρ_u and δ are positive numbers.
According to analysis presented in [11], the Lemma 1 holds true if the PID gains are appropriately chosen, and the on-line tuning algorithm (29) is able to obtain appropriate gains for the PID controller designed for a second order nonlinear system e.g., (2), which has been proved in [15]. For more details, please refer to [11]. Based on Lemma 1, a Lyapunov function candidate is chosen as:

$$V(E) = V_p(E_1) + \|F(e - \dot{a})\|_1. \tag{29}$$

Obviously, $V(E) > 0$ for any $E \neq 0$ and $V(E) = 0$ when $E = 0$. The derivative of (29) can be expressed as follows:

$$\dot{V}(E) = \dot{V}_p(E_1) + (\dot{e} - \ddot{a}) F \mathrm{sgn}(e - \dot{a}). \tag{30}$$

From (28) and (30), we obtain:

$$\begin{aligned} \dot{V}(E) \leq & fu - \rho_E \|E_1\|^2 - \rho_u \|u\|^2 \\ & + (\dot{e} - \ddot{a}) F \mathrm{sgn}(e - \dot{a}) \end{aligned}. \tag{31}$$

By substituting (14) into (31) and using the fact $u = \dot{p} - \dot{q}_d = \ddot{a} - \dot{e}$, we obtain:

$$\begin{aligned}\dot{V}(E) \leq & (\ddot{a} - \dot{e}) F \mathrm{sgn}(\sigma - \dot{a} - H\ddot{a}) - \rho_E \|E_1\|^2 \\ & - \rho_u \|u\|^2 + (\dot{e} - \ddot{a}) F \mathrm{sgn}(e - \dot{a})\end{aligned} . \quad (32)$$

Considering $\sigma - \dot{a} - H\ddot{a} = e - \dot{a} + H(\dot{e} - \ddot{a})$, (32) becomes

$$\begin{aligned}\dot{V}(E) \leq & H(\dot{e} - \ddot{a}) \frac{F}{H} [\mathrm{sgn}(e - \dot{a}) - \mathrm{sgn}(e - \dot{a} + H(\dot{e} - \ddot{a}))] \\ & - \rho_E \|E_1\|^2 - \rho_u \|u\|^2 \\ \leq & - \rho_E \|E_1\|^2 - \rho_u \|u\|^2 \leq 0\end{aligned} . \quad (33)$$

Therefore, the stability of the proposed control method is proved. Note that the following relation has been used in the above equation

$$y^T X [\mathrm{sgn}(z + y) - \mathrm{sgn}(z)] \geq 0, \quad (34)$$

where $X > 0$, and $y, z \in R$.

IV. EXPERIMENTAL EVALUATION

A. Experimental Setup

The experiment platform is shown in Fig. 3. The one degree of freedom orthosis is driven by a brushless DC motor. The whole actuator can provide a output torque up to 18 Nm approximately. The orthosis is equipped with an incremental encoder that measures the knee joint angle and the angular velocity is derived numerically.

In this experiment, the electromyography(EMG) signals of the Vastus Medialis, a muscle from the knee extensor group, are used to evaluate the influence of the human torque τ_h. The EMG signals are acquired using an EMG sensor (Delsys, USA). The raw EMG signals are processed with the following steps: a fourth-order high-pass Butterworth filter at 30Hz; elimination of the measurement noise; full-wave rectification.

The parameters in the experiments are chosen as follows:

- PID: $K_p = 300, K_i = 2, K_d = 7$
- APID:$K_p = 300, K_i = 2, K_d = 7, \lambda = 30$
- PSMC:$K_p = 300, K_i = 2, K_d = 7, H = 0.5$
- APSMC: $K_p = 300, K_i = 2, K_d = 7, \lambda = 30, H = 0.5$

B. Tracking performance and robustness

To verify the improvement of the tracking performance of the proposed control method, three groups of experiments were carried out to compare the tracking precision and robustness using different control methods. First, a given sinusoidal trajectory with the amplitude of 0.6 rad and the period of 1 s was used as the reference trajectory and four different control methods (PID, APID, PSMC and APSMC) were used to control the orthosis. The experiments were conducted on two healthy subjects whose relevant information like age, weight and height are listed in Table 1. The subjects were asked to sit on the table wearing the orthosis and not deliver any effect on the knee joint level (i.e., $\tau_h = 0$). The tracking angle and error of the two subjects are shown in Fig. 4 and Fig. 5, respectively. Furthermore, the adaptive

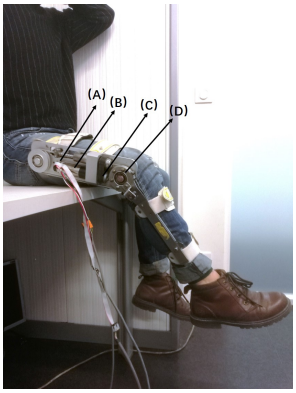

Fig. 3. The human lower limb and orthosis. (A)Incremental encoder. (B)Brushless DC motor. (C)Gear motor. (D)Pulley revolute knee joint.

PID gains variations are shown in Fig. 6. Experiment results show that APID and APSMC improve the tracking accuracy compared to PID and PSMC with both subject A and subject B. With the same controller parameters, the APSMC is able to maintain its tracking performance with respect to different subjects, while PID and PSMC have a decline in tracking accuracy. This can also be verified by the RMSE (root-mean-square error), which is summarized in Table 2. In the second experiment, subject A was asked to active his Vastus Medialis to actuate the knee joint in the opposite direction with the movement of orthosis, which can be regarded as an external disturbance of system (1). The EMG signal shown in Fig. 7(a) has an increasing amplitude of 0.03 mV and 0.02mV at the 2th second and the 3th second, respectively, which indicates that the subject force is against the orthosis movement, and an external disturbance is added in the system (1) as well. The results show that the APSMC is robust with respect to external disturbances and only a small error (0.2 rad) is caused by the human torque (see Fig.7(b) and Fig.7(c)).

TABLE I

SUBJECTS' SEX,AGE,WEIGHT,HEIGHT

Subject	Sex	Age	Weight(kg)	Height(cm)
A	male	24	58	172
B	male	31	63	180

C. Safety Test

In order to evaluate the safety of the shank-orthosis system by using the proposed APSMC controller, experiments of tracking a pre-defined discontinuous trajectory are carried out. As shown in Fig. 8, the desired trajectory is set as a sinusoidal function before 2.5s and then changes to a constant value of -0.2 rad. The sudden change of the desired trajectory indicates the large tracking error which results from the abnormal operation such as sudden lose of sensors data. The tracking results are shown in Fig. 8. The experiment results show that with a reasonable high value of H, the system using APSMC and PSMC can achieve a smooth and

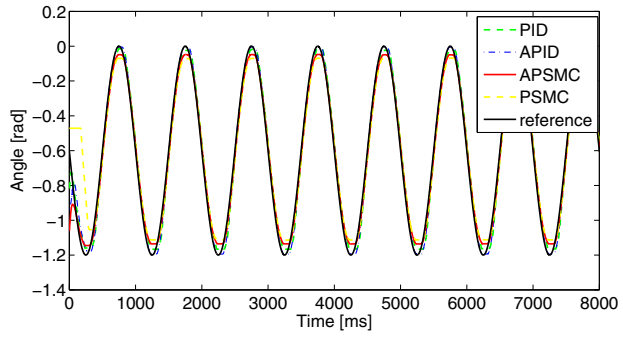

(a)

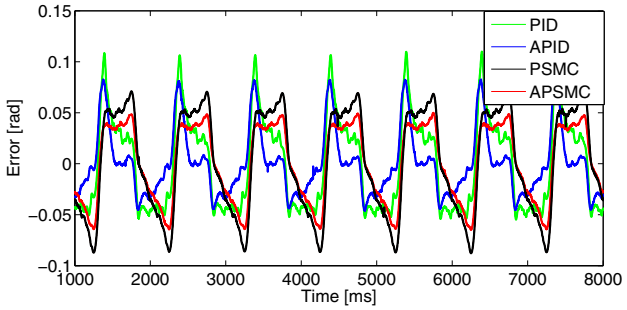

(b)

Fig. 4. Sinusoidal trajectory tracking results using PID, APID, PSMC and APSMC with subject A. (a) Tracking angle. (b) Tracking error.

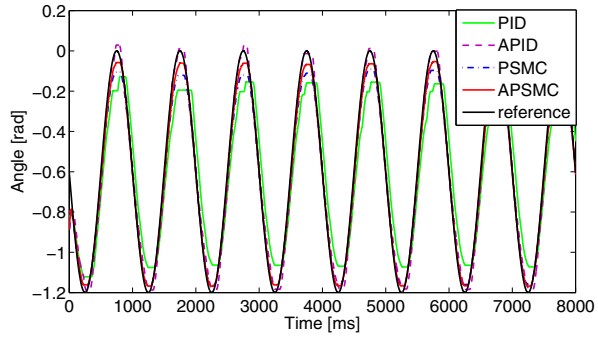

(a)

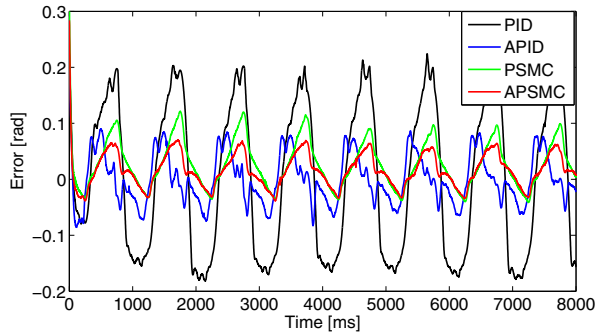

(b)

Fig. 5. Sinusoidal trajectory tracking results using PID, APID, PSMC and APSMC with subject B. (a) Tracking angle. (b) Tracking error.

TABLE II

RMSEs USING DIFFERENT CONTROL METHODS.

RMSE (rad) Subject \ Controller	APSMC	PSMC	APID	PID
A	0.0375	0.0483	0.0318	0.0453
B	0.0322	0.0505	0.0440	0.1380

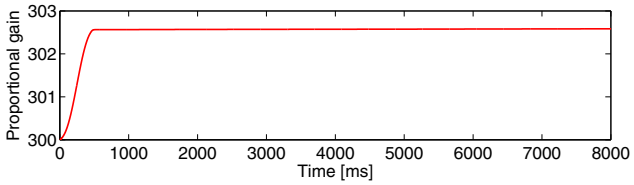

(a)

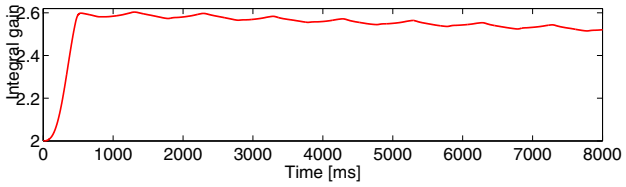

(b)

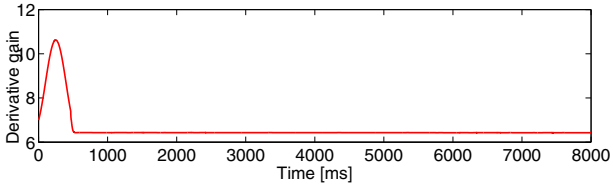

(c)

Fig. 6. Variations of proportional, integral and derivative gains. (a) Proportional gain. (b) Integral gain. (c) Derivative gain variation.

safe tracking towards desired value when large tracking error occurs, while overshot response is exerted using PID and APID, which may cause damage to the wearer.

The behavior of APSMC can be explained as, in situations of normal tracking, that is the tracking error is small and the proxy is on the sliding surface, the value of H hardly influences control performance, instead, the tracking performance is mainly determined by adaptive PID control. Thus, the system's response can slow down by setting a proper parameter H in the presence large tracking error, while good tracking performance is not affected in normal situations. Most traditional control methods is not able to achieve both at the same time. PID control, for instance, can achieve an smooth recovery without overshoot from large tracking error by increasing the velocity feedback gain, but this can also magnify the noise, which deteriorates the tracking accuracy.

V. CONCLUSIONS

Orthoses are effective in helping lower limb movement disordered patients to regain their athletic ability. Safety is crucial for this human-robot interact system. However, most of the control method is not able to ensure both safety and good tracking performance. In this study, a new APSMC

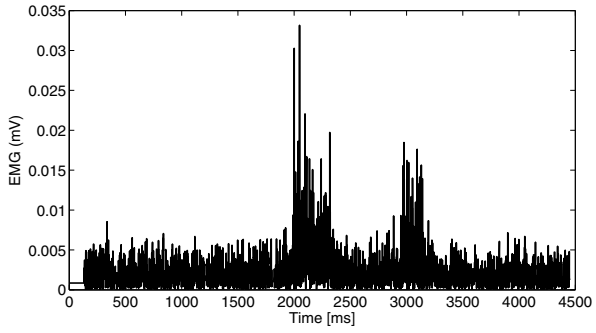

(a)

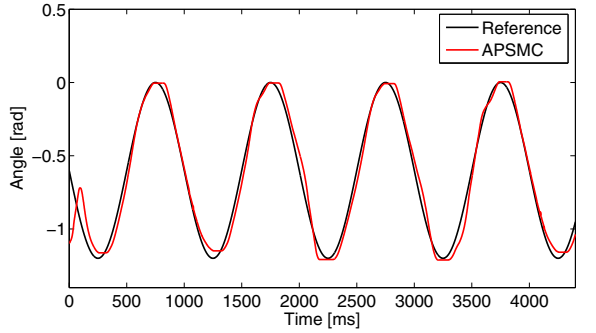

(b)

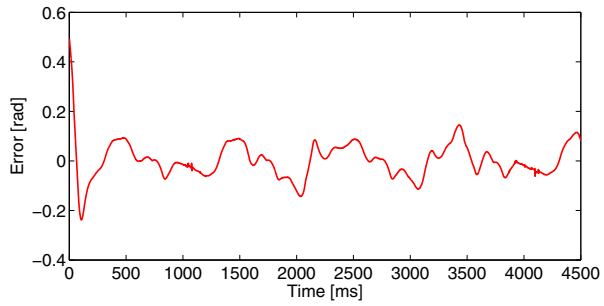

(c)

Fig. 7. Sinusoidal trajectory tracking experiment with human force ($\tau_h \neq 0$) using APSMC. (a) EMG signal. (b) Tracking result. (c) Tracking error.

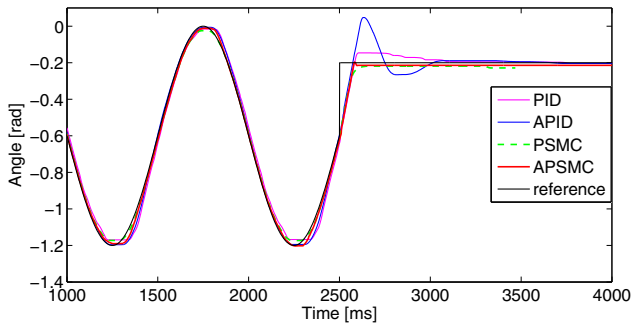

Fig. 8. Safety test.

is proposed for tracking control of knee joint orthosis. The proposed APSMC introduces a suitable adaptation method into the conventional PSMC so that the PID gains are self-tuning parameters. Thus, APSMC is more robust than the traditional PSMC. The comparison experiments using four different control method are conducted on two healthy subjects. The robustness to human force is illustrated by using EMG sensors. The experiment results show that APSMC improves the tracking accuracy and robustness with respect to the parameter uncertainties and external disturbances, compared to the standard PSMC. At the same time, APSMC has a smoother response than traditional stiff control in the presence of large tracking error, which guarantee the safety of the robot.

REFERENCES

[1] J. E. Pratt, B. T. Krupp, C. J. Morse, and S. H. Collins, "The roboknee: an exoskeleton for enhancing strength and endurance during walking," in *IEEE International Conference on Robotics and Automation, 2004. Proceedings. ICRA*, 2004, pp. 2430–2435 Vol.3.

[2] P. M. Bonutti, G. A. Marulanda, M. S. Mcgrath, M. A. Mont, and M. G. Zywiel, "Static progressive stretch improves range of motion in arthrofibrosis following total knee arthroplasty," *Knee Surgery Sports Traumatology Arthroscopy*, vol. 18, no. 2, pp. 194–199, 2010.

[3] C. Schmitt and P. Mtrailler, "A study of a knee extension controlled by a closed loop functional electrical stimulation," 2004.

[4] C. Fleischer, C. Reinicke, and G. Hommel, "Predicting the intended motion with emg signals for an exoskeleton orthosis controller," in *Ieee/rsj International Conference on Intelligent Robots and Systems*, 2005, pp. 2029–2034.

[5] S. Mohammed, W. Huo, J. Huang, H. Rifai, and Y. Amirat, "Nonlinear disturbance observer based sliding mode control of a human driven knee joint orthosis," *Robotics and Autonomous Systems*, vol. 75, pp. 41–49, 2017.

[6] W. Huo, S. Mohammed, and Y. Amirat, "Observer-based active impedance control of a knee-joint assistive orthosis," in *IEEE International Conference on Rehabilitation Robotics*, 2015, pp. 313–318.

[7] H. Rifai, S. Mohammed, B. Daachi, and Y. Amirat, "Adaptive control of a human-driven knee joint orthosis," in *IEEE International Conference on Robotics and Automation*, 2012, pp. 2486–2491.

[8] M. Van Damme, B. Vanderborght, B. Verrelst, R. Van Ham, F. Daerden, and D. Lefeber, "Proxy-based sliding mode control of a planar pneumatic manipulator," *The International Journal of Robotics Research*, vol. 28, no. 2, pp. 266–284, 2009.

[9] R. Kikuuwe and H. Fujimoto, "Proxy-based sliding mode control for accurate and safe position control," in *IEEE International Conference on Robotics and Automation (ICRA)*, 2006, pp. 25–30.

[10] B. Vanderborght, B. Verrelst, R. V. Ham, F. Daerden, and D. Lefeber, "Proxy-based sliding mode control of a planar pneumatic manipulator," *International Journal of Robotics Research*, vol. 28, no. 2, pp. 266–284, 2009.

[11] R. Kikuuwe, S. Yasukouchi, H. Fujimoto, and M. Yamamoto, "Proxy-based sliding mode control: a safer extension of pid position control," *IEEE Transactions on Robotics*, vol. 26, no. 4, pp. 670–683, 2010.

[12] J. Huang, W. Huo, W. Xu, S. Mohammed, and Y. Amirat, "Control of upper-limb power-assist exoskeleton using a human-robot interface based on motion intention recognition," *IEEE Transactions on Automation Science and Engineering*, vol. 12, no. 4, pp. 1257–1270, 2015.

[13] B. Badreddine, A. Zaremba, J. Sun, and F. Lin, "Active damping of engine idle speed oscillation by applying adaptive pid control," SAE Technical Paper, Tech. Rep., 2001.

[14] F. Lin, R. D. Brandt, and G. Saikalis, "Self-tuning of pid controllers by adaptive interaction," in *Proceedings of the American Control Conference*, vol. 5, 2000, pp. 3676–3681.

[15] B. M. Badreddine and F. Lin, "Adaptive pid controller for stable/unstable linear and non-linear systems," in *Proceedings of the 2001 IEEE International Conference on Control Applications (CCA)*, 2001, pp. 1031–1036.